

Mass transfer from a giant star to a main sequence companion and its contribution to long-orbital-period blue stragglers

Xuefei Chen^{1*} and Zhanwen Han¹

¹*National Astronomical Observatories/Yunnan Observatory, CAS, Kunming, 650011, P.R.China*

15 April 2008

ABSTRACT

Binary population synthesis shows that mass transfer from a giant star to a main-sequence (MS) companion may account for some observed long-orbital period blue stragglers. However, little attention is paid to this blue straggler formation scenario as dynamical instability often happens when the mass donor is a giant star. In this paper, we have studied the critical mass ratio, q_c , for dynamically stable mass transfer from a giant star to a MS companion using detailed evolution calculations. The results show that a more evolved star is generally less stable for Roche lobe overflow. Meanwhile, q_c almost linearly increases with the amount of the mass and angular momentum lost during mass transfer, but has little dependance on stellar wind. To conveniently use the result, we give a fit of q_c as a function of the stellar radius at the onset of Roche lobe overflow and of the mass transfer efficiency during the Roche lobe overflow.

To examine the formation of blue stragglers from mass transfer between giants and MS stars, we have performed Monte Carlo simulations with various q_c . The simulations show that some binaries with the mass donor on the first giant branch may contribute to blue stragglers with q_c obtained in this paper but will not from previous q_c . Meanwhile, from our q_c , blue stragglers from the mass transfer between an AGB star and a MS companion may be more numerous and have a wider range of orbital periods than those from the other q_c .

Key words: binaries:close -stars:evolution - blue stragglers

1 INTRODUCTION

Blue stragglers (BSs) are stars that have remained on the main sequence for a time exceeding that expected, for their masses, from standard stellar evolution theory. The existence of BSs indicates an incomplete understanding of stellar evolution and also of star formation within clusters (Stryker 1993). Since they are bright and blue, these objects may affect the integrated spectra of their host clusters by contributing excess spectral energy in the blue and ultraviolet. BSs are therefore important in studies of population synthesis (Xin & Deng 2005). Much evidence shows that these strange objects are relevant to primordial binaries (Ferraro et al. 2003; Davies, Piotto & Angeli 2004; Mapelli et al. 2004). Binary coalescence from a contact binary is a popular hypothesis for single BSs and it is believed that these contact binaries are mainly from case A

mass transfer ¹ (Mateo et al. 1990; Pols & Marinus 1994; Andronov et al. 2006; Chen & Han 2008). Mass transfer is another channel to produce BSs from primordial binaries. During Roche lobe overflow (RLOF), the less massive star accretes some material and goes upward along the main sequence, if it is still a main-sequence star. The accreting component may then be observed as a BS when it is more massive than the turnoff of the host cluster (Mc Crea 1964; Chen & Han 2004). Previous studies show that both case A and case B mass transfer are only responsible for some short- and mid-period BSs (Leonard 1996;

¹ According to the evolutionary state of the primary at the onset of mass transfer, three mass transfer cases are defined, i.e. case A for the primary being on the main sequence, case B for the primary after the main sequence but before central He burning, and case C for the primary during or after central He burning (Kippenhahn & Weigert 1967).

* xuefeichen717@hotmail.com

Chen & Han 2004), which are rare in some old open clusters, and case C mass transfer may account for BSs in long-orbital period spectroscopic binaries. During RLOF, the orbital period will decrease at first, however, if the primary continues to transfer material to the companion after the primary is less massive than the secondary, the binary will become wider and the orbital period will increase. Since dynamical instability often happens when the mass donor is a giant star, there is little work to focus on for this channel to BSs.

As is well known, a fully convective star will increase in radius with mass loss and decrease in Roche lobe radius if it is more massive than its accreting companion (Paczynski 1965). This means that the mass donor will overflow its Roche lobe by an ever-increasing amount, leading to mass transfer on a dynamical time-scale, the formation of a common envelope (CE) and a spiral-in phase. The critical mass ratio (the mass donor /the accretor) is about $2/3$ from a polytropic model with a polytropic index $n = 1.5$ for conservative mass transfer, indicating that mass transfer would be dynamically unstable if the mass donor has a mass larger than $2/3$ of the mass of the companion star. If stellar wind is not included before RLOF to decrease the primary's mass, case C mass transfer is always dynamically unstable for a binary with initial mass ratio $q_i > 1$ ² ($q_i = M_{1i}/M_{2i}$, M_{1i} and M_{2i} are the **initial** masses of the primary and of the secondary, respectively), and **therefore makes no contribution to BSs**. However, there are some problems when we use the **above criterion** in a real binary system for the following facts. (1) Giant stars have large condensed cores (usually they are degenerate), so they cannot be modelled by a fully convective star. The critical mass ratio increases substantially because of the condensed core (Hjellming & Webbink 1987). They conform to the formula as follows (Webbink 1988):

$$q_c = 0.362 + \frac{1}{3(1-M_c/M_1)}, \quad (1)$$

where M_c and M_1 are **the core mass and the total mass, respectively, of the donor as RLOF begins**. (2) The condition for dynamical instability also depends on the amount of mass and angular momentum loss during RLOF. Assuming that the lost mass carries away the same specific angular momentum as pertains to the mass donor, Soberman et al. (1997) gave a fitted Roche lobe mass-radius exponent $\zeta_L = -1.7\beta + (2.4\beta - 0.25)q$, where β is mass transfer efficiency determined as the mass fraction of the lost mass from the primary accreted by the secondary. We **may then** obtain the critical mass ratio q_c by setting the adiabatic mass-radius exponent $\zeta_S = \zeta_L$, where ζ_S can be fitted from the data of **numerical calculations** of Hjellming & Webbink (1987) and Soberman et al. (1997) (see also Han et al. 2001). Fig. 1 clearly shows the dependence of q_c on the mass transfer efficiency β . (3) Stellar wind prior to RLOF, which will be strongly enhanced due to the tidal interaction with the companion, will increase the core fraction in equation (1) and allow the system to **stabilize** more easily.

Possibly, a more fundamental problem of such a crite-

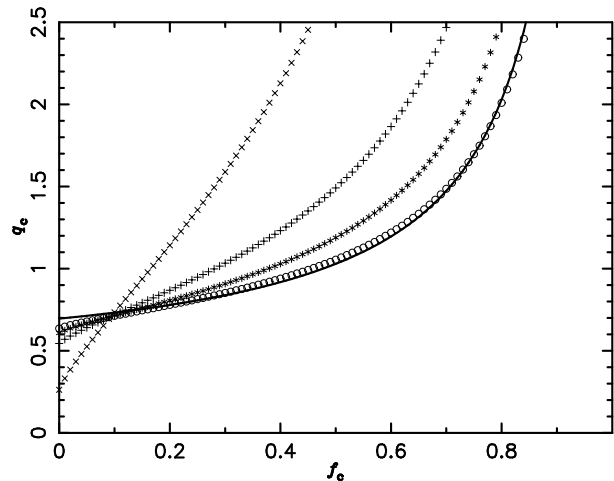


Figure 1. Critical mass ratio q_c for dynamically unstable RLOF. f_c is the core mass fraction of the mass donor. The cross, plus, asterisk and circle lines are for mass transfer efficiency $\beta = 0.25, 0.5, 0.75$ and 1.0 , respectively. The lost mass is assumed to carry away the same specific angular momentum as pertains to the mass donor. The solid line is from Webbink (1988) (see equation (1), $f_c = M_c/M_1$) for conservative RLOF.

riion is that it does not take into account the detailed dynamics of the mass transfer process. There are some systems, **observationally**, which should experience dynamical mass transfer while appearing to avoid a CE phase (Podsiadlowski et al. 1992). Several recent full binary evolution calculations also show that the simplistic criterion above is not really appropriate. For example, it is shown by Podsiadlowski et al. (2002) that mass transfer is dynamically stable for all giants up to a mass of about $2M_\odot$, in the case of giants transferring mass to a neutron star of $1.3/1.4M_\odot$. The study of Han et al. (2002) showed that q_c may be up to about 1.3 as $\beta = 0$.

In this paper, we will study the critical mass ratio for dynamical stability in mass transfer from a giant star to a main sequence companion from detailed binary evolutions, and adopt the results to estimate the contribution to BSs from the mass transfer. In section 2, we simply describe the numerical codes we have employed **in the study**. **The results** of the critical mass ratio are shown in section 3. In section 4, we show some examples of binaries which eventually form long orbital period BSs. The consequences from Monte Carlo simulations are shown in section 5. Discussions and conclusions are given in section 6.

2 BINARY EVOLUTION CALCULATIONS

The binary evolution code we employed was originally developed by Eggleton (1971; 1972; 1973), which has been updated with the latest input physics over the last three decades as described by Han et al. (1994) and Pols (1995; 1998). Some characteristics of the code, i.e. a self-adaptive non-Lagrangian mesh, the treatment of both the convective and semi-convective mixing as diffusion processes, the simultaneous and implicit solution of both the stellar structure equations and the chemical composition equations, etc. make the code very stable and easy to use. The current code

² The primary should be more massive than the secondary initially from standard stellar evolution if we expect the binary to be composed of a giant star and a main-sequence companion.

uses an equation of state that includes pressure ionization and Coulomb interaction, recent opacity tables derived from Rogers & Iglesias (1996) and Alexander & Ferguson (1994) (see Chen & Tout, 2007), nuclear reaction rates from Caughlan et al. (1985) and Caughlan & Fowler (1988), and neutrino loss rates from Itoh et al. (1989; 1992).

The ratio of mixing length to the local pressure scale-height $\alpha = l/H_p$ is set to 2, which fits to the Sun (Pols et al. 1998). Convective overshooting is included by incorporating a condition that mixing occurs in a region with $\nabla_r > \nabla_a - \delta_{ov}/(2.5 + 20\xi + 16\xi^2)$, where ξ is the ratio of radiative pressure to gas pressure and δ_{ov} is a specified constant. $\delta_{ov} = 0.12$ gives the best fit to the observed systems (Schröder et al. 1997), which corresponds to an overshooting of about $0.25H_p$. RLOF is included from the boundary condition

$$\frac{dm}{dt} = C \text{Max}[0, (\frac{r_{star}}{r_{lobe}} - 1)^3], \quad (2)$$

where r_{star} and r_{lobe} are the radii of the mass donor and its Roche lobe, respectively. dm/dt gives the mass loss rate of the primary, and C is a constant. In our study, we set $C = 500M_\odot \text{yr}^{-1}$, with which RLOF proceeds steadily and the lobe-filling star overfills its Roche lobe as necessary but never overfills its lobe by much, typically $(r_{star}/r_{lobe} - 1) < 0.001$.

If mass transfer is non-conservative, i.e. β is less than 1.0, some matter will **be lost** from the system, taking away some angular momentum. In our study, the accretor is a main-sequence star, and it is much **more compact** than a giant. So we assume that the lost mass carries away the same specific angular momentum as pertains to that of the accretor, similar to the case of a compact component. The study of Beer et al. (2007) shows that this assumption is appropriate for main-sequence components.

We only follow the evolution of the primary (initially more massive component) in a binary system when we study the critical mass ratio, since the structure of the primary is the main factor for the formation of CE in this phase. **We adopted the solar metallicity ($Z = 0.02$) in our calculations.** As we are mainly concerned with **BSs which originate from mass transfer**, only low- and intermediate-mass binaries are studied here. The initial mass of the primary increases from 1 to $8M_\odot$ by step of about $\Delta \log M/M_\odot = 0.1$ (i.e. $M_{1i} = 1.00, 1.26, 1.58, 2.00, 2.51, 3.20, 3.98, 4.95, 6.31$ and $7.94M_\odot$, respectively). When the mass donor evolves to **the** giant branch, it dramatically expands, and then its radius R may well represent the evolutionary phases. So we systematically vary the radius of the mass donor at the onset of RLOF³ and the mass of the companion star for each primary mass. If $M_{1i} < 2.00M_\odot$, the primary has a degenerate He core and undergoes a He flash as **the** central He is ignited. Before the He flash, the star can approach a very high luminosity as well as a very large

³ The radius of the primary at the onset of RLOF is actually its Roche lobe R_{cr1} , since the primary is just filling of its Roche lobe at that time. If the mass ratio q is given, the corresponding initial orbital separation A can be calculated from $R_{cr1}/A = 0.49q^{2/3}/[0.6q^{2/3} + \ln(1 + q^{1/3})]$ (Eggleton, 1983). For convenience, we only show the radius of the primary at the onset of RLOF in this paper.

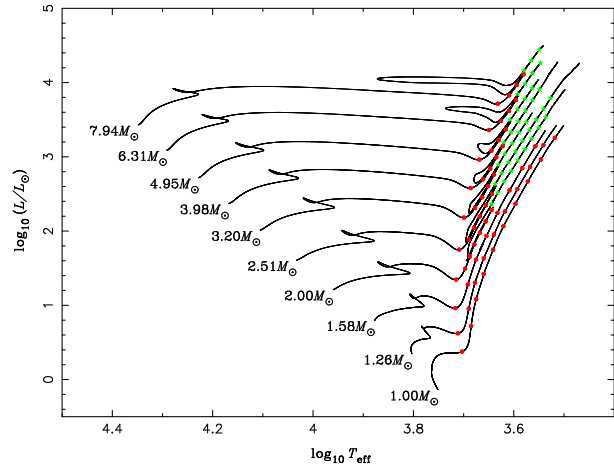


Figure 2. Evolutionary tracks for single stars from 1 to $8M_\odot$. For primaries in binary systems, the dots (for FGB) and asterisks (for AGB) indicate their positions at the onset of RLOF we studied in the paper. Corresponding stellar radii are presented in Table 1. The AGB cases for $M_1 < 2M_\odot$ are not plotted to ensure the distinction of the figure.

radius. So we choose an increase of the radius $\Delta \log R/R_\odot$ by **steps** of 0.2 from the base of the first giant branch (FGB) to the tip of **the** FGB to study the critical mass ratio. When $M_{1i} \geq 2.00M_\odot$, He burns quietly in the center and the radius difference of the primary from the base to the tip of FGB is not very large. We therefore set $\Delta \log R/R_\odot = 0.1$ for this case.

If a star has not **filled** its Roche lobe before central He burning, it will not **fill** its Roche lobe **during** He burning, because the star will contract after He ignition. We **therefore** have not considered the He-burning phase in the studies. After the exhaustion of **its** central He, the star expands again and its radius may become larger than that at the tip of **the** FGB. If $M_{1i} \geq 2M_\odot$, we continue the study on **the** AGB when the stellar radius equals to that at the tip of **the FGB**, and increase the radius by **steps** of $\Delta \log R/R_\odot = 0.1$. Fig. 2 shows the positions of the primaries as RLOF begins, corresponding stellar radii are presented in Table 1.

If $M_{1i} < 2M_\odot$, the code breaks down when the He flash occurs. To investigate the case on **the** AGB for a mass donor with $M_1 < 2.0M_\odot$, we constructed some stellar models after **the** He flash. Considering that some of the mass donors on **the** AGB may have evolved from some initially more massive stars⁴, we choose the point at the minimum stellar radius at the tip of **the** FGB for stars with $M_{1i} \geq 2M_\odot$ (i.e. $\log R/R_\odot = 1.41$) to start our studies and increase the radius by **steps** of $\Delta \log R/R_\odot = 0.1$. The stellar radii and corresponding q_c are listed in Table 2.

Table 1. Critical mass ratio for stable RLOF. M_{10} is ZAMS mass for the primary; $\log R$ is the radius of the primary at the onset of RLOF, q_c is the critical mass ratio and β is the fraction of the mass lost from the primary accreted by the secondary.

M_{10} M_\odot	$\log R$	q_c $\beta=0.0$	q_c $\beta=0.5$	q_c $\beta=1.0$	M_{10} M_\odot	$\log R$	q_c $\beta=0.0$	q_c $\beta=0.5$	q_c $\beta=1.0$	M_{10} M_\odot	$\log R$	q_c $\beta=0.0$	q_c $\beta=0.5$	q_c $\beta=1.0$
1.00	0.3048	1.3943	1.1927	1.0607	2.51	0.9785	1.4614	1.2539	1.0886	2.51	1.6653	1.2490	1.0574	0.8920
	0.5133	1.2477	1.0546	0.8933		1.0867	1.2757	1.0842	0.9279		1.7653	1.2183	1.0303	0.8670
	0.7133	1.2416	1.0530	0.8918		1.1867	1.2366	1.0473	0.8894		1.8653	1.1900	1.0032	0.8415
	0.9133	1.2615	1.0709	0.9066		1.2867	1.2138	1.0263	0.8655		1.9653	1.1535	0.9674	0.8079
	1.1133	1.2642	1.0719	0.9040		1.3867	1.1945	1.0087	0.8492		2.0653	1.1176	0.9325	0.7774
	1.3133	1.2545	1.0595	0.8902		1.4867	1.1759	0.9999	0.8341		2.1653	1.0847	0.9002	0.7471
	1.5133	1.2228	1.0312	0.8660							2.2653	1.0639	0.8776	0.7259
	1.7133	1.1901	0.9968	0.8324	3.20	1.2151	1.5982	1.3970	1.2560	3.20	2.3653	1.0512	0.8652	0.7168
	1.9133	1.1403	0.9561	0.7958		1.3236	1.3360	1.1371	0.9678		2.4653	1.0340	0.8505	0.7053
	2.1133	1.1131	0.9257	0.7696		1.4236	1.2672	1.0765	0.9128					
						1.5236	1.2200	1.0338	0.8738		1.7076	1.2668	1.1075	0.9235
						1.6236	1.1852	1.0029	0.8449		1.8076	1.1989	1.0138	0.8534
											1.9076	1.1650	0.9814	0.8237
											2.0076	1.1236	0.9417	0.7880
1.26	0.4110	1.3598	1.1588	1.0411	3.98	1.4407	1.7427	1.5413	1.3747	3.98	2.1076	1.0871	0.9059	0.7549
	0.6194	1.2172	1.0215	0.8658		1.5492	1.3730	1.1754	1.0029		1.8793	1.2251	1.0347	0.8737
	0.8194	1.2226	1.0272	0.8685		1.6492	1.2796	1.0892	0.9238		1.9793	1.1827	0.9992	0.8413
	1.0194	1.2341	1.0433	0.8783		1.7492	1.2172	1.0308	0.8713		2.0793	1.1399	0.9581	0.8043
	1.2194	1.2266	1.0360	0.8704		1.8492	1.1704	0.9880	0.8305		2.1793	1.1023	0.9205	0.7683
	1.4194	1.2089	1.0174	0.8532							2.2793	1.0647	0.8804	0.7356
	1.6194	1.1704	0.9814	0.8208							2.3793	1.0394	0.8570	0.7116
	1.8194	1.1289	0.9399	0.7835	4.94	1.6671	1.7617	1.5597	1.3637	4.94	2.0583	1.2105	1.0198	0.8628
	2.0194	1.0871	0.8983	0.7471		1.7756	1.3747	1.1770	1.0033		2.1583	1.1619	0.9792	0.8249
						1.8756	1.2719	1.0823	0.9161		2.2583	1.1201	0.9392	0.7870
						1.9756	1.1952	1.0116	0.8512		2.3583	1.0823	0.9013	0.7524
											2.4613	1.0438	0.8737	0.7201
											2.5613	1.0051	0.8461	0.6878
											2.6613	0.9674	0.8186	0.6553
1.58	0.5715	1.3634	1.1602	1.0055	6.31	1.9044	1.7582	1.5419	1.3578	6.31	2.2613	1.1864	0.9971	0.8392
	0.7800	1.2090	1.0225	0.8649		2.0129	1.3547	1.1576	0.9844		2.3613	1.1438	0.9622	0.8090
	0.9800	1.2047	1.0098	0.8535		2.1129	1.2563	1.0689	0.9034		2.4613	1.0985	0.9177	0.7686
	1.1800	1.2094	1.0202	0.8583		2.2129	1.1548	0.9740	0.8178		2.5613	1.0651	0.8841	0.7357
	1.3800	1.1908	1.0053	0.8441										
	1.5800	1.1629	0.9760	0.8162										
	1.7800	1.1174	0.9310	0.7764										
	1.9800	1.0771	0.8886	0.7393	7.94	2.1091	1.6967	1.4669	1.2748	7.94	2.4438	1.1624	0.9764	0.8201
						2.2176	1.2971	1.1004	0.9288		2.5438	1.1235	0.9418	0.7913
						2.3176	1.2306	1.0457	0.8804		2.6438	1.1019	0.9203	0.7700
						2.4176	1.1247	0.9476	0.7924					
1.91	0.7239	1.3905	1.1847	1.0165	2.00	1.4175	1.2764	1.0819	0.9130	2.00	1.6653	1.2490	1.0574	0.8920
	0.9324	1.2140	1.0269	0.8695		1.5175	1.2661	1.0730	0.9063		1.7653	1.2183	1.0303	0.8670
	1.1324	1.1971	1.0078	0.8504		1.6175	1.2388	1.0474	0.8805		1.8653	1.1900	1.0032	0.8415
	1.3324	1.1816	0.9977	0.8369		1.7175	1.2068	1.0171	0.8526		1.9653	1.1535	0.9674	0.8079
	1.5324	1.1652	0.9803	0.8217		1.8175	1.1698	0.9816	0.8210		2.0653	1.1176	0.9325	0.7774
	1.7324	1.1223	0.9387	0.7838		1.9175	1.1329	0.9470	0.7890		2.1653	1.0847	0.9002	0.7471
						2.0175	1.0971	0.9090	0.7546		2.2653	1.0639	0.8776	0.7259
					2.00	2.1175	1.0901	0.9045	0.7462	2.00	2.3653	1.0512	0.8652	0.7168
						2.2175	1.0734	0.8844	0.7313		2.4653	1.0340	0.8505	0.7053
2.00	0.7672	1.3710	1.1779	1.0065	2.00	1.4175	1.2764	1.0819	0.9130	2.00	1.6653	1.2490	1.0574	0.8920
	0.8759	1.2447	1.0530	0.9035		1.5175	1.2661	1.0730	0.9063		1.7653	1.2183	1.0303	0.8670
	0.9757	1.2261	1.0298	0.8745		1.6175	1.2388	1.0474	0.8805		1.8653	1.1900	1.0032	0.8415
	1.0757	1.2039	1.0157	0.8614		1.7175	1.2068	1.0171	0.8526		1.9653	1.1535	0.9674	0.8079
	1.1757	1.1980	1.0093	0.8521		1.8175	1.1698	0.9816	0.8210		2.0653	1.1176	0.9325	0.7774
	1.2757	1.1890	1.0030	0.8446		1.9175	1.1329	0.9470	0.7890		2.1653	1.0847	0.9002	0.7471
	1.3757	1.1786	0.9936	0.8355		2.0175	1.0971	0.9090	0.7546		2.2653	1.0639	0.8776	0.7259
					2.00	2.1175	1.0901	0.9045	0.7462	2.00	2.3653	1.0512	0.8652	0.7168
						2.2175	1.0734	0.8844	0.7313		2.4653	1.0340	0.8505	0.7053

3 THE CRITICAL MASS RATIO FOR A GIANT MASS DONOR

As mentioned in section 1, dynamically unstable RLOF often occurs when the mass donor is a giant at the onset of mass transfer. Fig. 3 shows the mass transfer rate vs the mass of the primary for a typical binary undergoing dynamical unstable mass transfer. The primary is $1.00M_\odot$ with a core mass $M_c = 0.344M_\odot$ at the onset of RLOF, and $\beta = 0$

during the RLOF. From the figure we see that mass transfer initially occurs on a thermal time-scale. The mass transfer rate, \dot{M} , rises quickly to a level of $10^{-5}M_\odot\text{yr}^{-1}$ at first and continues to grow more slowly later. After the primary has lost about $0.04M_\odot$ (point A), the system encounters dynamical instability. The behaviour here is similar to that of radiative mass donors with a mass ratio greater than 3 (Han & Podsiadlowski 2006), but it cannot be explained by the evolution of the entropy profile as in the case of a mass donor with a radiative envelope. It is related to the evolution of binary parameters, which strongly depend on the angular momentum loss associated with the mass loss from the system. Furthermore, in comparison to the delayed dynamical

⁴ For example, a star with $M_{1i} > 2M_\odot$ becomes less than $2M_\odot$ because of stellar wind, then the star has not passed through a phase with a high radius before He burning.

Table 2. Critical mass ratio for stable RLOF for AGB mass donors with mass less than $2M_\odot$. M_1 is the mass of the primary, $\log R$ is the radius of the primary at the onset of RLOF, q_c is the critical mass ratio and β is the fraction of the mass lost from the primary accreted by the secondary.

$\log R$	$M_1 = 1.00M_\odot$			$M_1 = 1.26M_\odot$			$M_1 = 1.60M_\odot$		
R_\odot	$\beta = 0.$	$\beta = 0.5$	$\beta = 1.$	$\beta = 0.$	$\beta = 0.5$	$\beta = 1.$	$\beta = 0.$	$\beta = 0.5$	$\beta = 1.$
1.4096	2.0406	1.7919	1.5816	1.7504	1.4589	1.2640	1.5018	1.3020	1.1192
1.5096	1.9040	1.6705	1.4550	1.5912	1.3709	1.2294	1.4360	1.2290	1.0533
1.6096	1.8061	1.5761	1.3728	1.5302	1.3154	1.1481	1.3954	1.1904	1.0157
1.7096	1.7154	1.4891	1.3096	1.4791	1.2676	1.0833	1.3617	1.1608	0.9834
1.8096	1.6223	1.4045	1.2144	1.4142	1.2078	1.0256	1.3059	1.1100	0.9362
1.9096	1.5773	1.3260	1.1437	1.3544	1.1529	0.9759	1.2575	1.0629	0.8940
2.0096	1.4503	1.2448	1.0076	1.2937	1.0970	0.9228	1.2058	1.0146	0.8486
2.1096	1.3590	1.1681	0.9986	1.2307	1.0382	0.8698	1.1540	0.9631	0.8053
2.2096	1.2955	1.1014	0.9327	1.1827	0.9904	0.8290	1.1167	0.9290	0.7730
2.3096	1.2553	1.0649	0.8849	1.1562	0.9658	0.8057	1.0976	0.9094	0.7542

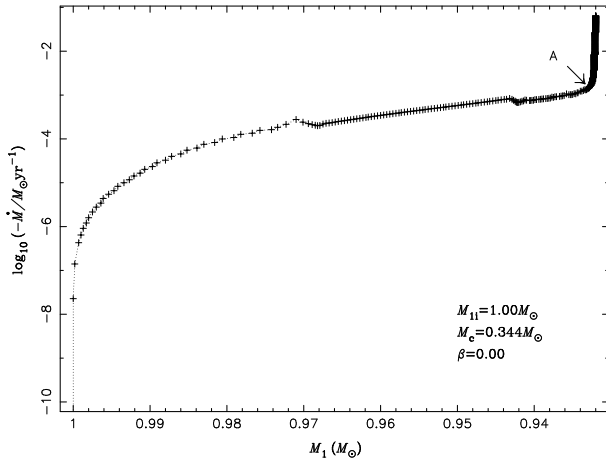


Figure 3. Mass transfer rate vs the primary mass for a binary of $M_{1i} = 1.00M_\odot$. Mass transfer efficiency $\beta = 0.0$ and the core mass is $0.344M_\odot$. Point A gives the place at which mass transfer dramatically increases because of dynamical instability.

cal instability in the radiative mass donor, the primary with a convective envelope here loses much less mass during the delayed time and probably has little **influence** on the final **outcome**.

The results of our calculations are summarized in Tables 1 and 2. For each ZAMS, we present the radius of the primary $\log R/R_\odot$ at the onset of RLOF and the critical mass ratio q_c for dynamically stable RLOF from different mass transfer efficiency β . The results demonstrate that RLOF is **probably** dynamically stable even if the mass donor is more massive than the secondary for $\beta < 1$. In particular, when the mass donor is less than $2M_\odot$ and fills its Roche lobe on **the** AGB, RLOF may be dynamically stable even for $\beta = 1$. Since the core is not very degenerate and the envelope is not fully convective when the star is at or near the base of **the** FGB, q_c is much larger at the base of **the** FGB than in the following evolutionary phases for each β .

Figs. 4 and 5 present q_c vs $\log R/R_\odot - A_0$ for **low-mass and intermediate-mass binaries**, respectively, when the mass donors are on the FGB. Here A_0 is **the log of the radius of the primary at the base of the FGB**. We

include the result of $M_{1i} = 1.9M_\odot$ in Fig. 4 (see also Table 1). The results for the mass donor on **the** AGB are showed in Figs. 6 and 7. In all of the figures, we see that a more evolved star (with a larger stellar radius at the onset of RLOF) is less stable for RLOF, especially when the mass donor is on **the** AGB at the onset of mass transfer. The reasons are as follows. For more evolved binaries, the evolutionary time-scale is shorter and hence the mass transfer rate higher than those for the less-evolved ones. However q_c is non-monotonic initially in Fig.4 because the core is not very degenerate and the envelope is not yet full convective in this phase.

The cases at the last point on **the** FGB and at the first point on **the** AGB give a different tendency as described above, since the two points are on different giant branches, and **the stars have different cores, i.e. a non-degenerate He core on the FGB while a possibly degenerate CO core on the AGB**. Meanwhile, the degree of convection is also different at the two points.

As shown in Fig.5, there is a threshold for q_c when the initial primary mass $M_{1i} = 3.98M_\odot$. When $M_{1i} \leq 3.98M_\odot$, q_c systematically increases with the initial primary's mass while it is opposite when $M_{1i} \geq 3.98M_\odot$. This phenomena is likely revelant to the degenerate degree of the core. We examined the degeneracy parameter ψ in the calculations and found that ψ becomes negative just at $M_{1i} = 3.98M_\odot$.

We know that, when central He is exhausted in a star, there **exists** a He-burning shell and a H-burning shell. The H-burning shell extinguishes first when it burns outwards, and then the He-burning shell also extinguishes. The star begins to contract and the temperature increases until H is ignited. With the increase of temperature, He is also ignited but in a very thin shell. The He ignition in a very thin shell is unstable, **and** leads to a **dramatic** expanding of the star. After the expansion, He-burning becomes stable and the star then has two stable burning shells again, and so on. This behaviour is known as **the** thermal pulse. The thermal pulse may result in a sharp increase of mass transfer rate and leads dynamical instability **to be more likely to occur** such as in Fig. 8. In principle, if the mass donor has two burning shells, the thermal pulse will likely affect the final results. For the cases we studied, however, the influences seem **small** and can be neglected.

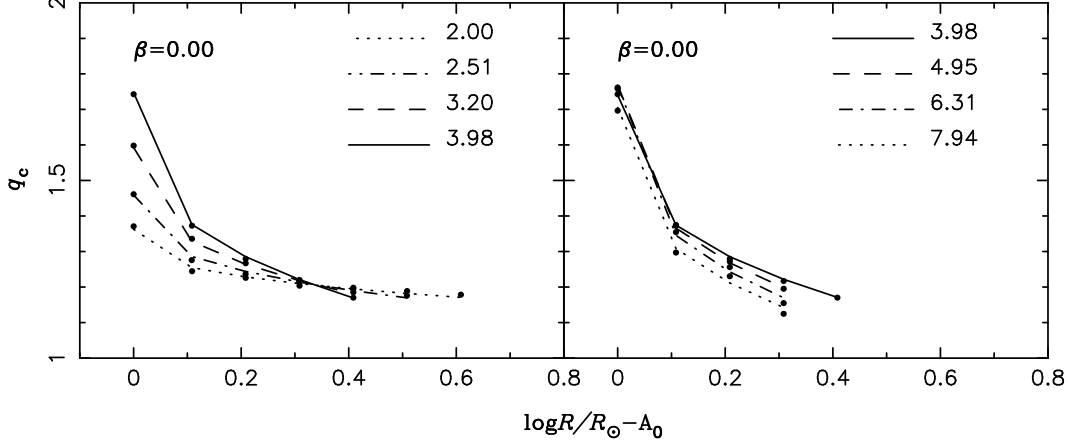


Figure 5. Similar to figure 4, but for intermediate-mass binaries, i.e. $M_{1i} = 2.00, 2.50, 3.20, 4.00, 5.00, 6.30$ and $8.00 M_{\odot}$. The lines are from equations (5) and (6).

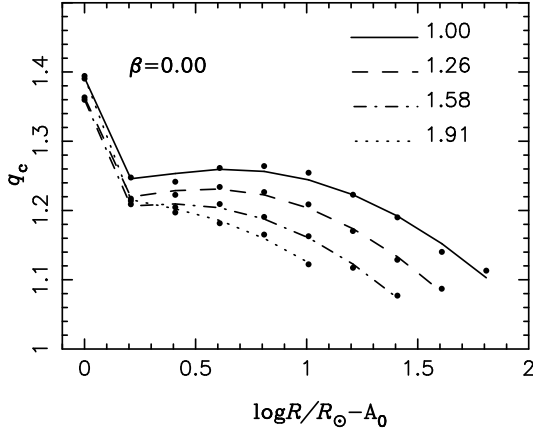


Figure 4. Critical mass ratio for low-mass binaries of FGB+MS, i.e. $M_{1i} = 1.00, 1.26, 1.60$ and $1.90 M_{\odot}$. The lines are from the fitting formulae of equations (4) to (6).

To simply use this results, we fitted q_c from our calculations. The influence from β is nearly linear and can be fitted as

$$q_c = q_{c0} - c_0\beta, \quad (3)$$

For the FGB,

$$q_{c0} = c_1 + c_2(\log R/R_{\odot} - A_0) + c_3(\log R/R_{\odot} - A_0)^2, \quad (4)$$

when $M_{1i} < 2.00 M_{\odot}$ and $\log R/R_{\odot} - A_0 > 0.2$. In other cases,

$$q_{c0} = c_4 + c_5(\log R/R_{\odot} - A_0)^{1/3}. \quad (5)$$

Here

$$c_i = c_{i,1} + c_{i,2}M_1 + c_{i,3}M_1^2. \quad (6)$$

The values of $c_{i,j}$ and c_0 are listed in Table 3 for different cases.

For the case of the AGB,

$$q_{c0} = c_1 + c_2(\log R/R_{\odot} - A_0) + c_3(\log R/R_{\odot} - A_0)^2. \quad (7)$$

The coefficients c_i and c_0 are listed in Table 4. One may send a request to xuefeichen717@hotmail.com for the

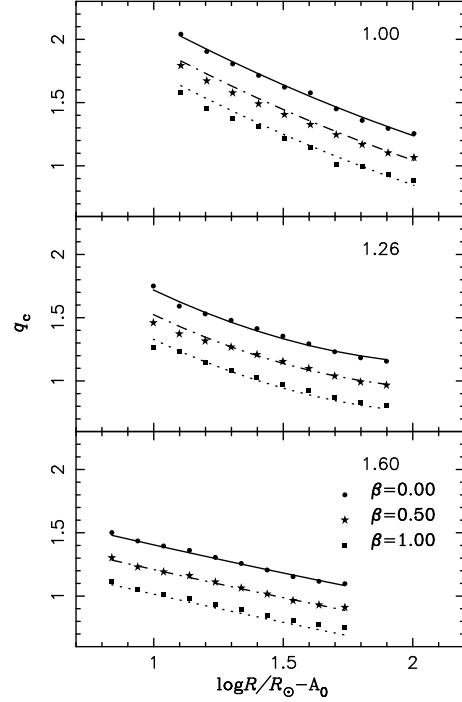


Figure 6. Critical mass ratio for low-mass binaries when the primary is on the AGB. The lines are from the fitting formulae of equations (6) and (7).

FORTTRAN code of all the formulae used in this paper.

To compare with the results of the polytropic model, we present the dependence of q_c on the core mass M_c as well as on the core mass fraction f_c for low-mass binaries in Fig. 9, ignoring the points at the base of the FGB for each mass. Here the core mass is defined as the mass within the hydrogen mass fraction less than 0.1⁵. From the figure, we

⁵ It is a little bit difficult to determine the core in a real star as described in the polytropic model. However, the core mass defined here is a close approximation to that defined in the polytropic model.

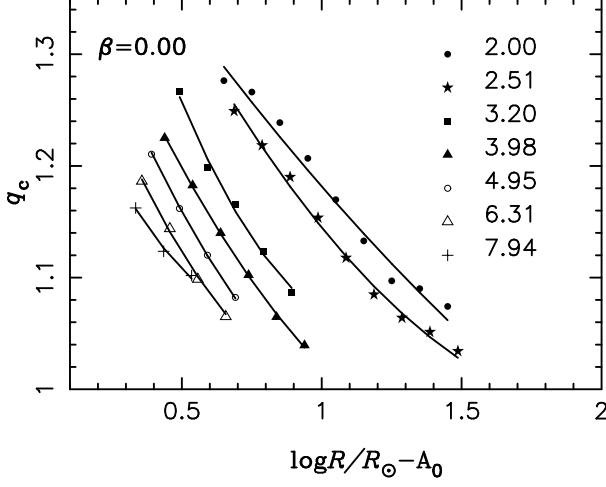


Figure 7. Critical mass ratio for intermediate-mass binaries when the primary is on the AGB. The lines are from the fitting formulae of equations (6) and (7).

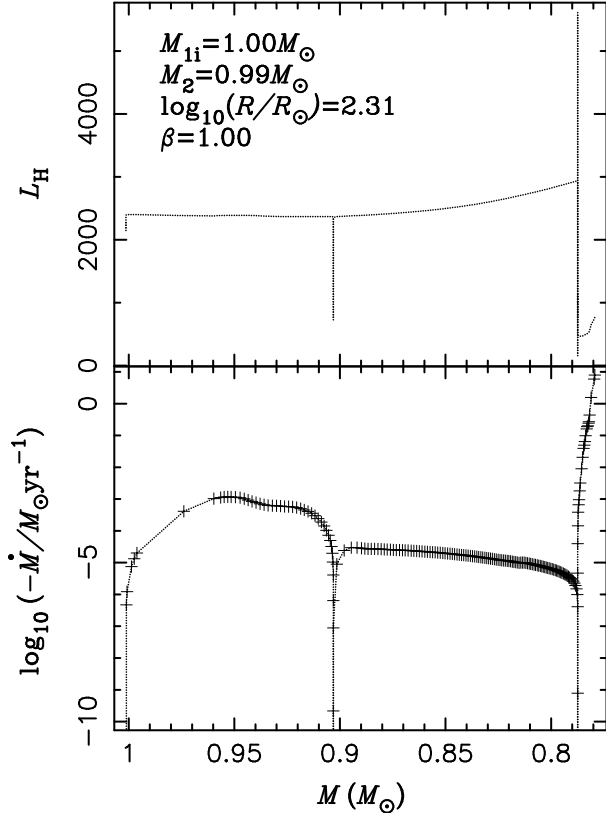


Figure 8. Mass transfer rate as well as H-burning luminosity vs the primary mass for a binary when the mass donor is on the AGB.

see a clear relation between q_c and M_c , but not between q_c and f_c . q_c may be fitted as follows:

$$q_c = q_{c0} - 0.35\beta \quad (8)$$

where

$$q_{c0} = 1.142 + 1.081M_c - 2.852M_c^2. \quad (9)$$

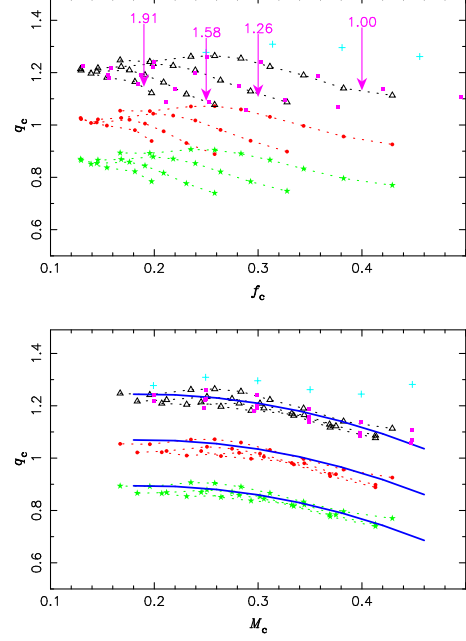


Figure 9. The dependencies of critical mass ratio q_c on the core mass fraction f_c and on the core mass M_c for low-mass binaries, i.e the initial primary mass $M_{1i} = 1.00, 1.26, 1.6$ and $1.9M_\odot$, respectively. The triangles, dots and asterisks are for mass transfer efficiency $\beta = 0, 0.5$ and 1.0 , respectively. The squares and pluses are from Han et al (2002), where stellar wind is included before RLOF and $\beta = 0$. The pluses are for binaries with a primary mass equal to $0.8M_\odot$, and the squares for $M_{1i} \geq 1.00M_\odot$. The solid lines in the bottom panel are from equations (8) and (9).

Table 3. The coefficients $c_{i,j}$ and c_0 for various cases when the mass donor is on the FGB (from equations(7) to (10)). Here $r = \log R/R_\odot - A_0$.

cases	i	$j = 1$	$j = 2$	$j = 3$	c_0
$M_1 < 2.00M_\odot$	1	1.4418	-0.3477	0.1180	0.37
&	2	-0.08252	0.4180	-0.1873	
$r \geq 0.2$	3	0.08967	-0.3129	0.1079	
$M_1 < 2.00M_\odot$	4	1.7141	-0.4919	0.1695	0.37
& $r < 0.2$	5	-0.3978	0.2620	-0.1101	
$M_1 \geq 2.00M_\odot$	4	0.9989	0.1755	0.003139	0.35
& $M_1 < 3.98M_\odot$	5	0.2740	-0.2353	-0.007348	
$M_1 \geq 3.98M_\odot$	4	1.3840	0.1389	-0.0124	0.37
	5	0.05596	-0.2602	0.02045	

The studies above have not included the influences from the stellar wind. Han et al. (2002) included the stellar wind prior to RLOF when they studied the q_c for low-mass binaries on the FGB and $\beta = 0$. We have included their results in Fig. 9. The pluses are for binaries with $M_{1i} = 0.8M_\odot$ ⁶

⁶ We have not studied the case for $M_{1i} = 0.8M_\odot$ in this paper, because the time-scale is too long for a star with this mass to evolve from zero-age main sequence to giant branch. **Meanwhile, it might be more likely that low-mass binaries (i.e the initial primary less than $1M_\odot$) contribute to blue**

Table 4. The coefficients $c_{i,j}$ and c_0 for various cases when the mass donor is on the AGB.

cases	i	$j = 1$	$j = 2$	$j = 3$	c_0
$M_1 < 2.51M_\odot$	1	1.0462	0.3115	-0.03702	0.34
	2	-0.6179	0.5193	-0.2027	
	3	0.7346	-0.7568	0.2074	
$M_1 \geq 2.51M_\odot$ &	1	-0.5270	1.4289	-0.2325	0.36
	2	7.1432	-4.9954	0.7625	
$M_1 < 3.98M_\odot$	3	-4.9258	3.2653	-0.4966	
$M_1 \geq 3.98M_\odot$	1	1.4681	0.01922	-0.004501	0.36
	2	0.1092	-0.2844	0.02368	
	3	-0.1971	0.1226	-0.006051	
$M_1 < 2.00M_\odot$	1	0.02442	7.0840	-3.6961	0.39
	2	9.6761	-19.0892	7.9462	
	3	-4.5199	7.8189	-3.1087	

and the squares for $M_{1i} \geq 1.00M_\odot$ (see Table 3 in their paper). We see that all the squares are well along the fitting line of $\beta = 0$, indicating that stellar wind has little influence on q_c . However, the mass ratio will decrease due to stellar wind, and RLOF will be more stable, e.g. the mass ratio possibly becomes less than q_c at the onset of RLOF and the binary will undergo a stable mass transfer. For the case of $M_{1i} = 0.8M_\odot$, q_c from Han et al. (2002) is obviously larger than the fitting value, which means that RLOF is more stable in binaries with this **primary** mass. Since the binaries with $M_{1i} = 0.8M_\odot$ have a larger f_c in comparison to those with $M_{1i} \geq 1.0M_\odot$ ⁷, the high q_c for $M_{1i} = 0.8M_\odot$ here likely indicates some contributions from f_c , as is possibly concealed by that from M_c for binaries with $M_{1i} \geq 1.00M_\odot$ (see the discussion in section 6).

4 EXAMPLES OF THREE BINARIES RESULTING IN BSS

In this section, we present the detailed evolutions for three binaries, which are selected mainly for the reason that we are interested in BSs in the old open cluster M67, where many BSs, including several long-period BSs, have been observed. M67 has a metallicity similar to that of the Sun (Hobbs & Thorburn 1991; Friel & Janes 1993). There are some researches on the age of M67. It may range from 3.2 ± 0.4 Gyr (Bonatto & Bica 2003) to 6.0 Gyr (Janes & Phelps 1994). The study of VandenBerg & Stetson (2004) derived an age of 4.0 Gyr. In the N-body model of this cluster (Hurley et al. 2005), the authors investigated the behaviour around 4 Gyr. So we also consider that its age is about 4 Gyr, indicating that the mass of

stragglers via coalescence induced by angular momentum loss (Chen & Han 2008), while not from the mass transfer between a giant and a MS.

⁷ In the study of Han et al. (2002), the mass donor has a similar core mass but a different stellar mass at the onset of RLOF. Therefore, a high stellar mass means a smaller core mass fraction f_c . See Table 3 in their paper for details.

the turnoff M_{to} is about 1.2 to $1.3M_\odot$, which is the main factor of the cluster we will consider as we choose the binary samples. Basic requirements for the binaries which may contribute to BSs in a cluster via a giant transferring mass to a MS companion are for the masses of both components, i.e. the primary should be more massive than the turnoff to ensure that it has left the main sequence and the secondary should be less than the turnoff if it is still on the main sequence at the cluster age. The fact that the secondary should accrete certain material before it becomes a BS will give a further constraint on the binary parameters. Obviously, $\beta = 0$ is ruled out since no material is accreted by the secondary in this case. In the following of this section, we will give three examples and present the evolutionary results in details.

Example 1: RLOF is dynamically stable for initial parameters. As shown in section 3, q_c decreases with the mass transfer efficiency β . This means that, in order to ensure that β is large enough to increase the secondary's mass to be larger than the turn-off, the mass ratio q should be as small as possible. However, q should be larger than unity to confirm that mass transfer occurs between a giant star and a MS companion. We therefore choose a binary of $1.3 + 1.2M_\odot$ ($q = 1.08$). Meanwhile, since the orbital period increases with the core mass (or the radius) of the mass donor at the onset of RLOF, a large core mass (or stellar radius) is necessary for long orbital period BSs. However, when $M_c > 0.4M_\odot$, q_c is less than 1.0 even for $\beta = 0$. We therefore set $M_c = 0.35M_\odot$ ($\log R/R_\odot = 1.7503$) at the onset of RLOF. From equations (8) and (9), $\beta = 0.16$ for $q_c = 1.08$. We then set $\beta = 0.1$ in the calculation.

Example 2: RLOF is dynamically unstable for initial parameters, but it will be stable after some mass loss of the primary by stellar wind prior to RLOF. Stellar wind is included only on the giant branch by the mode of Reimers' (1975):

$$\dot{M}_{\text{wind}} = 4 \times 10^{-13} \eta RL/M, \quad (10)$$

where η is a dimensionless factor. The same binary as example 1 was examined here but with $\beta = 0.5$. In general, η is 1/4 (Renzini 1981; Iben & Renzini 1983; Carraro et al. 1996). However it is expected by many authors that giant stars have much higher mass loss rates than that of Reimers, especially when the stars are far away from the base of giant branch (e.g. Bloeker 1995). Furthermore, tidal interaction between the two components of the binary also increases the mass loss rate. So we set $\eta = 2.5$ ⁸ in the calculation. When RLOF begins ($M_c = 0.355M_\odot$), $M_1 = 1.11M_\odot$ ($q = M_1/M_2 = 0.93$). We switch the stellar wind off once the mass transfer rate exceeds the value given by eq(10) and have not included it after RLOF. From eqs(8) and (9), we get $q_c = 0.99$ for $\beta = 0.5$ and $M_c = 0.35M_\odot$. So RLOF is dynamically stable as it begins.

Example 3: RLOF is dynamically unstable for initial parameters, but it becomes stable after the initially dynamically unstable mass transfer, if we assume that CE

⁸ We also examined the cases for $\eta = 1/4$ and 1, and found that both of them are too small to strip enough mass away to lead to $q < q_c$ as RLOF begins.

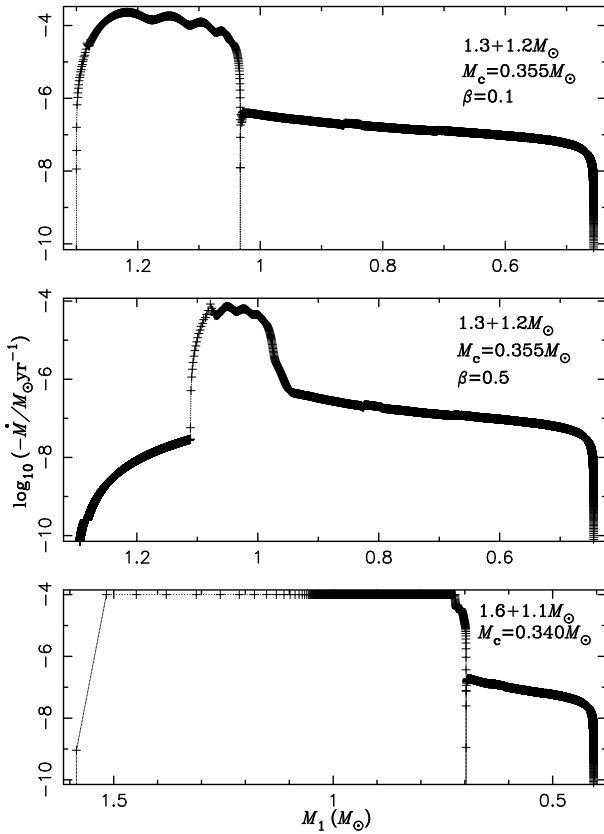


Figure 10. Mass loss rate vs the mass of the primary for the three binaries in the text. The system parameters are presented in each panel. Stellar wind is not included in panels (a) and (c), while it is included at the giant branch in panel (b) with the mode of Reimer ($\eta = 2.5$). During the initially dynamically unstable phase in panel (c), we set the highest mass loss rate of the primary to be $1 \times 10^{-4} M_{\odot} \text{yr}^{-1}$ (see the text for details).

has not developed during this phase according to the study of Beer et al. (2007). Beer et al. (2007) argued that a wide range of systems avoid CE phase because mass transfer is super-Eddington even for non-compact companions. The accretion energy released in the rapid mass-transfer phase strips away a large fraction of the giant’s envelope, reducing the tendency to dynamical instability and merging. More constraints are necessary to determine **whether** the CE is formed or not in this case, but we have little knowledge **about** it. For simplicity, we assume that CE has not developed in the binary we study here, i.e. in a binary with $1.6 + 1.1 M_{\odot}$. The code cannot work for the initial dynamically unstable mass transfer because of the high mass transfer rate \dot{M} . We therefore artificially limit the highest \dot{M} to be $1 \times 10^{-4} M_{\odot} \text{yr}^{-1}$, and the accretion rate of the secondary \dot{M}_a is equal to \dot{M} as $\dot{M} < 1 \times 10^{-5} M_{\odot} \text{yr}^{-1}$, and equal to $1 \times 10^{-5} M_{\odot} \text{yr}^{-1}$ as $\dot{M} \geq 1 \times 10^{-5} M_{\odot} \text{yr}^{-1}$. From this assumption, β ranges from 1.0 to 0.1, then to 1.0 again during the whole RLOF **period**. The maximum accretion rate of the MS companion here, i.e. $1 \times 10^{-5} M_{\odot} \text{yr}^{-1}$, is comparable with the typical value of symbiotic stars (Scott & Webbink 1984).

Figure 10 presents the mass loss rate to the total mass of the primary for the three binaries. In these figures we see that, after the initial rapid mass loss, the primary loses its

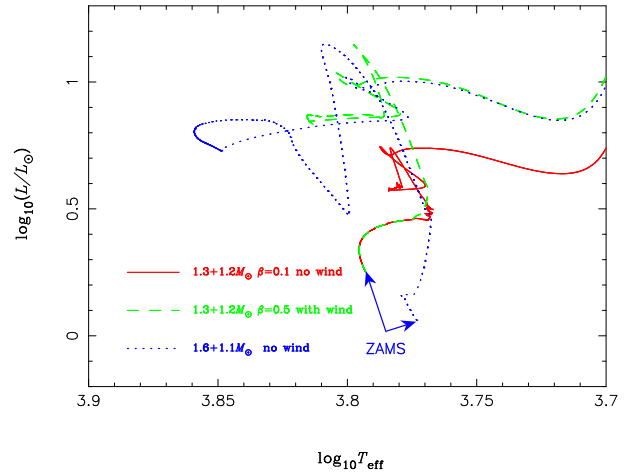


Figure 11. The evolutionary tracks for the secondaries of the three binaries we examined in the text.

material at a rate of about 10^{-6} to $10^{-8} M_{\odot} \text{yr}^{-1}$. Generally this slow mass transfer occurs after **the inversion of the mass ratio**, i.e. the primary is less massive than the secondary. During the slow mass transfer phase, the radius of the primary **again increases** but with a much lower level in comparison to that in the rapid mass loss phase. At the same time, the Roche lobe radius of the primary increases with mass loss, since the orbital period becomes longer and longer after the **inversion** of q . So if CE has not developed in the dynamically unstable phase in a binary such as example 3, it is very likely that CE will never develop in the binary. The material lost from the primary in this phase will **be lost** from **the** system in a way similar to stellar wind, and RLOF eventually terminates after most of the primary’s envelope is lost. Note that the mass loss of the system here is different from the ejection of CE. The former needs no orbital energy but the latter needs some. So binaries avoiding CE have long orbital periods.

The behaviours of the secondaries of the three binaries are presented in Fig. 11. Since the secondaries cannot **accrete** the mass from the primary in a very short time, they have left thermal equilibrium and evolve in a way similar to pre-MS stars during the initial phase instead of going upward along the main sequence. Due to **the** long orbital periods, the secondaries **do not overfill** their Roche lobes. They finally become normal main-sequence stars with a higher He fraction in the envelope when new thermal equilibrium is established, and evolve similarly to normal single stars with **those** masses. These rejuvenated stars have much longer timescales (including the phase of the secondaries with lower masses before accretion) on the main sequence and have the possibility to be BSs.

The main characteristics of the three binaries are listed in Table 5, from which we may obtain some clues on their parent binaries and evolutionary histories. For example, although the secondary in example 2 has a mass similar to that in example 3 after accretion, the latter is much bluer (Fig. 11) when both of them return to thermal equilibrium since the latter is much less evolved at the onset of RLOF. The two secondaries have different orbital periods, different compact components and different lifetimes etc., and appear in different age of the cluster, as shown in Table 5.

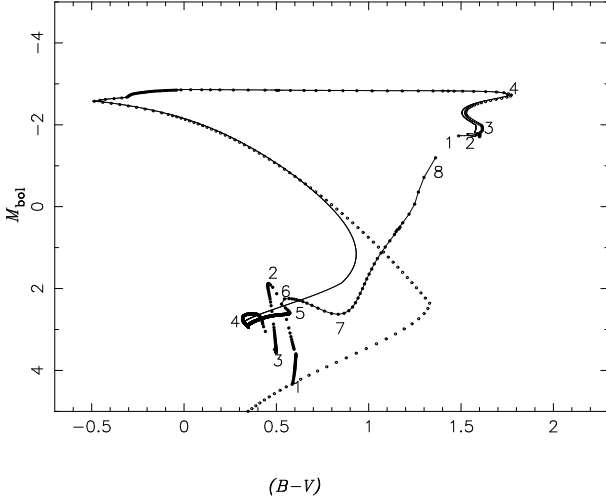


Figure 12. The colour and magnitude evolutions for the individual components of the binary $1.6 + 1.1M_{\odot}$ as well as for the whole system. The early evolutions of both components prior to RLOF are not plotted in the figure. The circle and dotted lines are for the primary and the secondary, respectively, and the solid line is the combination of the two components. **The numbers are the time sequences of the evolutions.**

As an example, we give a colour-magnitude diagram of both of the components as well as the binary system for example 3 in Fig.12. The combined colour and magnitude of the binary result from add-and-subtract calculations of the luminosity of both components (see Appendix A). The evolutions of the components prior to RLOF have no differences from a standard stellar evolution and are not plotted in the figure. During the whole mass transfer phase the system resembles the characteristics of the primary because the primary is much more luminous than the secondary, but the **timescale** is very short. Once the primary becomes **cooler**, i. e. less luminous than its component, the binary is hardly **distinguishable** from the main-sequence component. It is very difficult to find the clues from the compact component, even from **spectral** observations because of the long orbital period.

5 MONTE CARLO SIMULATION

To investigate BSs from mass transfer between giants and MS companions, we performed a Monte Carlo simulation for a sample of 10^6 binaries (very wide binaries are actually single stars). A single starburst is assumed in the simulation, i.e. all the stars have the same age and metallicity ($Z = 0.02$). The initial mass function (IMF) of the primary, the initial mass ratio distribution and the distribution of initial orbital separation are as follows:

- i) the IMF of Miller & Scalo (1979) is used and the primary mass is generated from the formula of Eggleton, Fitchett & Tout (1989):

$$M_1 = \frac{0.19X}{(1-X)^{0.75} + 0.032(1-X)^{1/4}} \quad (11)$$

where X is a random number uniformly distributed between 0 and 1. The mass ranges from 0.8 to $100M_{\odot}$.

- ii) the mass ratio distribution is quite controversial and,

for simplicity, we only consider a constant mass ratio distribution (Mazeh et al.1992).

$$n(q') = 1, 0 \leq q' \leq 1 \quad (12)$$

where $q' = 1/q = M_2/M_1$.

- iii) We assume that all stars are members of binary systems and the distribution of separations is constant in $\log a$ (**where** a is separation).

$$an(a) = \begin{cases} \alpha_{\text{sep}}(a/a_0)^m, & a \leq a_0 \\ \alpha_{\text{sep}}, & a_0 < a < a_1 \end{cases} \quad (13)$$

where $\alpha = 0.070$, $a_0 = 10R_{\odot}$, $a_1 = 5.75 \times 10^6 R_{\odot} = 0.13\text{pc}$ and $m = 1.2$. This distribution gives an equal number of wide binary systems per logarithmic interval and 50 per cent of systems with orbital periods less than 100 yr⁹ (Han et al. 1995).

The rapid binary evolution code developed by Hurley et al. (2000; 2002) is employed here. In addition to all aspects of single-star evolution, this code includes many features of binaries, i.e. mass transfer, mass accretion, common-envelope evolution, collisions, supernova kicks and angular momentum loss mechanisms etc.. In particular, circularization and synchronization of the orbit by tidal interaction are calculated for convective, radiative and degenerate damping mechanisms. As a comparison, we adopt three **criteria** obtained in different ways, i.e. from a polytropic model (equation 1), from the paper of Hurley et al. (2002) and from this paper.

In the paper of Hurley et al. (2002),

$$q_c = [1.67 - x + 2(M_c/M)^5]/2.13, \quad (14)$$

where M_c and M are the core mass and the total mass of the donor, respectively, x is the exponent of the mass-radius relation at constant luminosity for giant stars and equals to 0.3. This criterion comes from the assumption that the adiabatic mass-radius exponent of a giant star $\zeta_{\text{ad}} = \partial \ln R / \partial \ln M$ equals to the Roche lobe mass-radius exponent ζ_L , where $\zeta_L \approx 2.13q - 1.67$ for conservative mass transfer (Tout et al. 1997) and $\zeta_{\text{ad}} \approx -x + 2(M_c/M)^5$, which is fitted from detailed stellar models.

From the sample, we obtain 303291 binaries which begin RLOF when the primary is a giant or more evolved star via Hurley's rapid binary evolution code. In the following **section** we will give the consequences from different **criteria** of the dynamical instability for mass transfer from a giant to a MS companion.

5.1 The results from Hurley's criterion

Among the 303291 binaries undergoing mass transfer from a giant or more evolved star to its companion, most of them

⁹ It is an assumed distribution inferred from observations of spectroscopic binaries (see a series of papers of Griffin, R. F in *The Observatory*). Indeed, there are many distributions used in the literature, but they are all flat for wide binaries, leading to similar binary population results. The important thing for the currently adopted distribution is that it implies 50 per cent of stellar systems with orbital periods less than 100 yr. One can simply multiply the results with a coefficient if another percentage is assumed.

Table 5. The characteristics for three different evolutionary examples in the text. η = the factor of Reimer’s wind, M_c = the core mass at the onset of RLOF, β = the mass fraction of the lost matter of the primary accreted by the secondary, t_{RLOF} = the age at the onset of RLOF, t_{MS} = the age of the secondary when it terminates its main sequence P_e , M_{1e} , M_{2e} are the orbital period, the mass of the primary and the mass of the secondary at the end of RLOF.

	binary M_\odot	stellar wind η	M_c M_\odot	β	P_e days	t_{RLOF} Gyrs	t_{MS} Gyrs	M_{1e} M_\odot	M_{2e} M_\odot
example 1	1.3+1.2	0.0	0.356	0.1	803	4.71	5.45	0.46	1.28
example 2	1.3+1.2	2.5	0.356	0.5	722	4.71	5.45	0.44	1.53
example 3	1.6+1.1	0.0	0.340	-	439	2.47	4.57	0.41	1.50

eventually experience CE evolution, **leaving** short-period binaries or mergers of the two components if the CE cannot be stripped away.¹⁰ According to **Hurley’s criterion**, only 3746 binaries may avoid CE formation and probably show the characteristics of some strange objects, e.g. symbiotic stars, BSs etc. during or after RLOF. Here we are concerned **with** the outcomes of BSs.

Most of the 3746 binaries which avoid CE formation begin RLOF when the primaries are on the giant branches, i.e. on the first giant branch (FGB) for 17 binaries, on the early asymptotic giant branch (EAGB, after central He burning but before the first thermal pulse) for 415 binaries, and on the thermally pulsing AGB (TPAGB) for 3295 binaries. The simulation shows that, 3139 binaries will pass through BS phase during their lives and 2208 of them have undergone dynamically stable RLOF before they become BSs¹¹. This means that RLOF is an important process to increase the secondary’s mass to be larger than the turnoff of a cluster. All the 2208 binaries have long orbital periods (greater than 1000 d) and their mass ratios are less than unity at the onset of RLOF, indicating that the primaries have lost most of their envelopes prior to RLOF (e.g. 2164 binaries have a mass donor being on TPAGB). As a consequence, the BSs from this way also have long orbital periods (greater than 1600 d).

At the age of 4 Gyr, we obtain 96 BSs. Fig. 13 presents the distribution of the orbital period as well as the mass ratio versus the mass for the 96 BSs. In the figure, we see that, though the mass ratio at the onset of BS phase is a little different, all the BSs have similar mass ratios (around 0.4) when they leave the main sequence. **We explain this as follows. BS formation from mass transfer between giants and MS companion has some constraints. For example, RLOF should be dynamically stable. For q_c adopted here, the primaries should be close to or on the TPAGB before 4 Gyr. Meanwhile, the secondary should be stay on the MS at 4 Gyr (the MS timescale of the secondary after RLOF is only in or-**

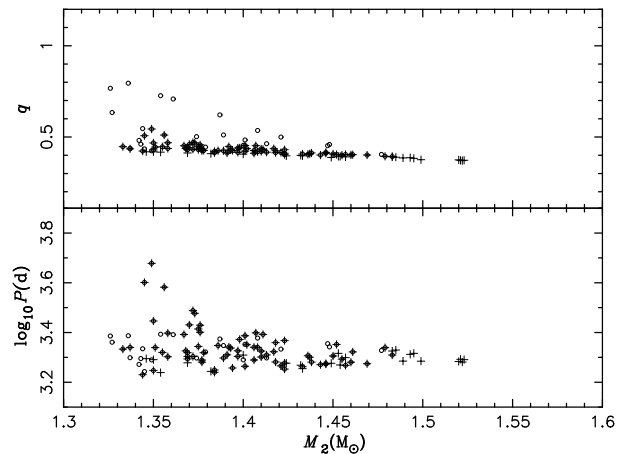


Figure 13. Mass ratio as well as orbital period versus the mass of the secondary for 96 binaries which fulfill $t_1 \leq 4\text{Gyr} < t_2$, where t_1 and t_2 are the ages at the onset and at the end of BSs, respectively. The circles are for the case at t_1 and the pluses are for the case at t_2 .

der of 10^8 yr). So the binaries which may produce BSs in this cluster are very similar initially, and the products after RLOF are also similar. The difference of q at the onset of BSs comes from the fact that RLOF has not terminated in these binaries at that time. Although RLOF still exists in some BSs, which results in the increase of their masses, the orbital period **do not show** obvious changes during the whole BS phase. All the BSs are near the turnoff of M67, indicating that this evolution channel, i.e mass transfer from a giant star to a main sequence companion (MS), can only account for the BSs in this region.

5.2 The results from the polytropic model’s criterion

Using the same binary sample, we examined the evolutionary consequence from the criterion of the polytropic model (see equation (1) in section 1). As discussed in the paper of Hurley et al. (2002), the value of q_c from the polytropic model is obviously larger than that of Hurley et al. (2002) with increasing core mass. For example, it is a factor of 2 larger at $M_c/M_1 = 0.6$. So more binaries may avoid dynamically unstable RLOF in the criterion of the polytropic model than those in the criterion of Hurley et al. (2002).

From equation 1, 8522 binaries avoid CE formation and

¹⁰ Because the primaries have left the main sequence, these mergers are different from those from two main-sequence components. They are giant stars and then have no contribution to single BSs.

¹¹ We included wind accretion in the code for the reason presented in section 6, so some BSs can be formed without RLOF. The simulation here indicates that wind accretion is important for BS formation, as the secondaries in some binaries cannot be larger than the turnoff mass without wind accretion even after RLOF.

5919 pass through the BS phase during their lives. Among of the 5919 binaries, 4287 have undergone or are just undergoing dynamically stable RLOF before the secondaries become BSs. At the age of 4 Gyr, we obtained 175 long-orbital period BSs (greater than 1600 d). The distribution of the orbital period as well as the mass ratio versus the mass for the 175 BSs are similar to those from the criterion of Hurley et al. (2002).

5.3 The results from this paper's criterion

Now we study the outcomes from the criterion in this paper. **Different from the two criteria above, we only evolve binaries to the onset of RLOF using Hurley's code and obtain the following evolutions from assumptions below.**

When we determine whether mass transfer leads to a BS formation or not in a certain cluster, two characteristic parameters of the secondary, i.e. the mass M_a and the MS lifetimes t_{MS} , are critical. The former is relevant to the initial mass of the secondary and the mass transfer efficiency β , while the latter is determined by the central H fraction and the total mass of the secondary after accretion. Meanwhile, the ages **at the onset and termination** of RLOF are also important. For example, RLOF should start before or at the cluster age $t_{cluster}$ to ensure that the secondary may accrete some matter, but it cannot stop much earlier than $t_{cluster}$, or the secondary has likely left the main sequence. Therefore, only the binaries, which complete mass transfer between $t_{cluster} - t_{MS}$ and $t_{cluster}$ as well as have secondary's mass $M_a > M_{to}$ during or after accretion, will contribute to BSs in a cluster. In fact, the mass transfer process from a giant star to its companion is on a very short time-scale (about 10^6 yr) in comparison to the MS time of the secondary after accretion, and then can be ignored. The amount of matter lost from the mass donor during RLOF and the mass transfer efficiency β finally determine how much matter is accreted by the secondary. From section 4, we see that the final mass of the mass donor after RLOF is a little larger (about $0.1M_\odot$) than the core mass at the onset of RLOF. Meanwhile, from the studies of the initial-final mass relation (Meng et al. 2007), the final mass of a star after RLOF or the super wind is around the core mass at the onset of RLOF or before super wind. The maximum difference induced by thermal pulses and mass loss is less than $0.4M_\odot$, so we choose a range of the final mass of the mass donor from M_c to $M_c + 0.4M_\odot$ to examine the characteristics of the secondaries and of the binary systems.

For M67 ($t_{cluster} = 4 \times 10^9$ yr), we obtained different possible candidates from various β for $t_{MS} = 1 \times 10^9$ yr and $t_{MS} = 5 \times 10^8$ yr, respectively¹². The final orbital period of the candidates is estimated based on the assumption

Table 6. The BS numbers in M67 obtained from FGB stars transferring matter to MS companions for various β . The MS timescale of the secondary after RLOF, t_{MS} , is set to 1×10^9 yr (from the 2nd to 5th columns) and 5×10^8 yr (from the 6th to 9th columns), respectively. The final masses of the primary are $M_{1f}^1 = M_c$, $M_{1f}^2 = M_c + 0.1M_\odot$, $M_{1f}^3 = M_c + 0.2M_\odot$ and $M_{1f}^4 = M_c + 0.4M_\odot$, where M_c is the core mass of the primary at the onset of RLOF.

β	M_{1f}^1	M_{1f}^2	M_{1f}^3	M_{1f}^4	M_{1f}^1	M_{1f}^2	M_{1f}^3	M_{1f}^4
0.1	414	412	406	371	319	317	311	276
0.2	169	169	169	169	150	150	150	150
0.3	31	31	31	31	30	30	30	30
0.4	2	2	2	2	2	2	2	2

Table 7. The BS numbers in M67 obtained from EAGB stars transferring matter to MS companions for various β .

β	M_{1f}^1	M_{1f}^2	M_{1f}^3	M_{1f}^4	M_{1f}^1	M_{1f}^2	M_{1f}^3	M_{1f}^4
0.1	58	56	52	38	32	30	28	18
0.2	48	47	46	37	41	40	39	30
0.3	29	29	29	29	28	28	28	28
0.4	13	13	13	13	13	13	13	13
0.5	1	1	1	1	1	1	1	1

that the lost matter carries off the specific angular momentum as the accretor. Tables 6 to 8 present the BS numbers for different mass donors, i.e. the mass donors are FGB stars (FGB+MS), EAGB stars (EAGB+MS) and TPAGB stars (TPAGB+MS), respectively. The corresponding distributions of the orbital period versus the final mass for various β are shown in Figs. 14 to 16.

We have not obtained BSs from an FGB star transferring matter to a MS companion in M67 from the **criteria** of Hurley et al. (2002) and of the polytropic model, since the mass donor has not lost much mass by wind prior to RLOF and the core mass is not very large. **Both of these facts make the condition $q < q_c$ difficult to fulfill** (see equations (1) and (14)). However, from the criterion of this paper, several BSs will be formed in M67 if $\beta \leq 0.4$. From Table 6, we see that β strongly affects the contribution to BSs from this evolutionary channel. A small β contributes more BSs because RLOF is stabilized more easily. The mass of the secondary in this case is generally large enough to be larger than the turnoff after accretion even as $\beta \leq 0.1$.

The contribution to BSs from EAGB+MS, in comparison to that of TPAGB+MS, is very small, although the value of q_c for EAGB+MS is likely larger than that of TPAGB+MS because of the small radii at the onset of RLOF. This is relevant to the mass loss by wind prior to RLOF during the two phases. The stellar wind is generally much less in EAGB than that in TPAGB. Our study indicates that the mass loss prior to RLOF during EAGB phase is usually not enough to make $q < q_c$, while **a lot of** matter in the envelope of the primary has left the system by wind prior to RLOF for binaries of TPAGB+MS. **So for systems of TPAGB+MS, the mass transfer is easily stabilized and leads to the formation of long-orbital period binaries after RLOF.**

¹² The MS time-scales here are referred to Table 5— **it is about 8×10^8 yr from the onset of RLOF to the termination of the secondary on the main sequence.** From Fig. 17, we see that the maximum mass ratio at the onset of RLOF is less than 1.2 for binaries resulting in BSs, which means that the secondary is only slightly less than the turn-off, and then the MS time-scale of the secondary after accretion will not be very long. Meanwhile, it is likely longer than 5×10^8 yr from Table 5.

Table 8. The BS numbers in M67 obtained from TPAGB stars transferring matter to MS companions for various β .

β	M_{1f}^1	M_{1f}^2	M_{1f}^3	M_{1f}^4	M_{1f}^1	M_{1f}^2	M_{1f}^3	M_{1f}^4
0.1	97	80	63	29	41	33	23	9
0.2	150	122	96	50	75	60	47	21
0.3	175	142	112	61	98	73	57	32
0.4	175	146	105	58	104	85	58	32
0.5	157	132	97	45	96	79	57	24
0.6	111	100	81	31	66	59	47	16
0.7	68	56	42	15	43	37	27	10
0.8	39	26	11	4	24	17	7	3
0.9	32	20	4	0	21	14	4	0
1.0	33	20	4	0	22	14	4	0

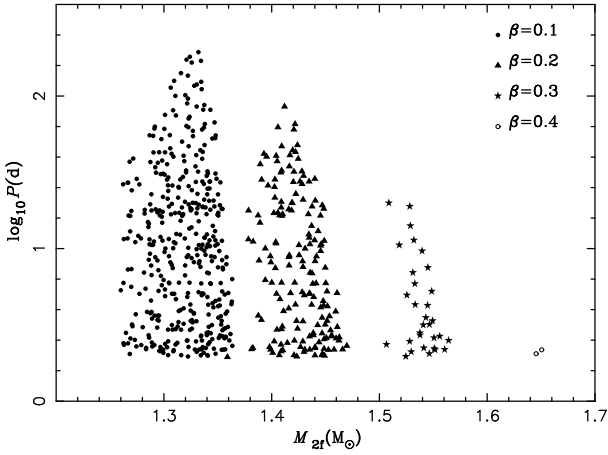


Figure 14. Orbital period versus mass for the BSs in M67 resulting from FGB stars transferring material to main-sequence companions. The final mass of the primary is assumed to be $M_c + 0.2M_\odot$, where M_c is the core mass of the mass donor at the onset of RLOF. See the text for the details.

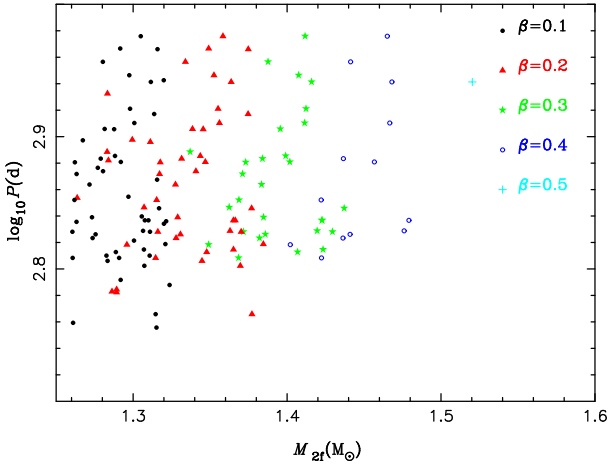


Figure 15. Similar to Fig. 14, but the mass donors are EAGB stars, i.e. after central He burning but before the first thermal pulse.

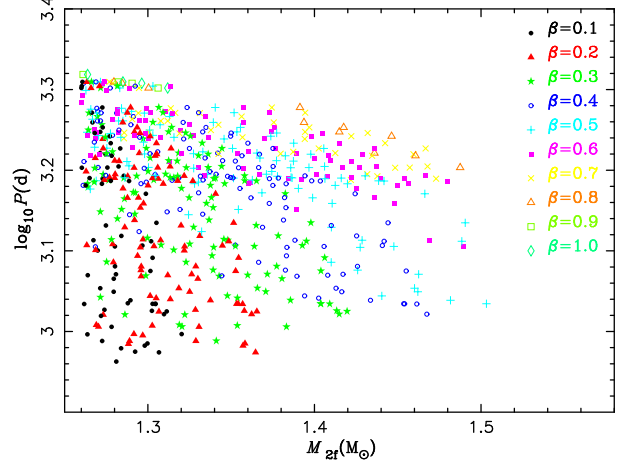


Figure 16. Similar to Fig. 14, but the mass donors are TPAGB stars.

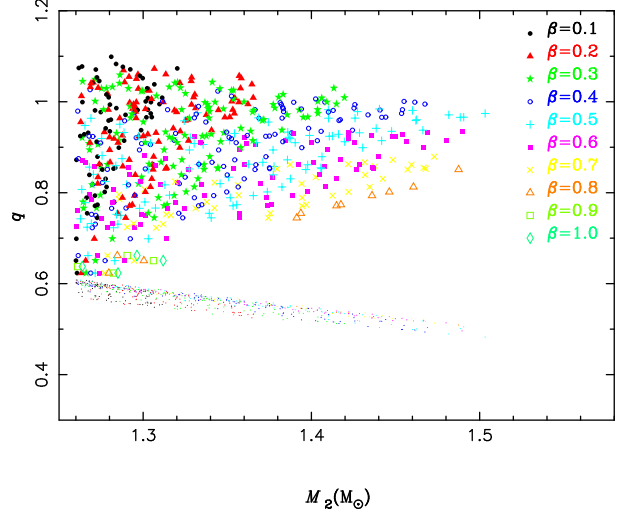


Figure 17. Mass ratio versus the mass for the BSs resulting from TPAGB stars transferring matter to MS companions for various β when the final mass of the primary is $M_{1f} = M_c + 0.2M_\odot$. The small dots are at the end of RLOF.

The influence of β on the BS formation from TPAGB+MS binaries is non-monotonic, i.e. the BS number first increases, and then decreases with the increase of β (see Table 8). This non-monotonic phenomenon is induced by the criterion of q_c and the mass of the MS companion after accretion. With the increase of β , q_c becomes smaller and smaller, which leads $q < q_c$ to be fulfilled **more unlikely**, but the MS companion may accrete more material from the primary to increase the mass to be larger than the turn-off of the cluster. The results of Table 8 indicate that, when $\beta \leq 0.4$, the mass of the MS companion is the main factor to determine the formation of BS from this way, but the dynamical instability is the crucial **factor** when $\beta > 0.4$.

From Fig. 14 we see that, for the BSs from mass transfer between an FGB star and a MS companion, their masses increase and the range of the orbital period becomes narrower (mainly some long orbital period BSs disappear) with the increasing β , since a large β means more matter ac-

creted by the secondary (leading to a larger final mass) and less angular momentum lost from the system (resulting in a shorter orbital period). Furthermore, a long-orbital period indicates a larger stellar radius at the onset of RLOF, and then a smaller q_c as shown in section 3. Therefore, with the increase of β , the RLOF in relatively long-orbital-period binaries firstly changes from dynamically stable to dynamically unstable, **and** directly leads to the disappearance of long-orbital-period BSs. The orbital period of the BSs from this **channel** has a wide range, i.e. from several days to hundreds of days for $\beta = 0.1$. However, BSs with $P \geq 100$ days can only be produced when $\beta \leq 0.2$ and their masses are near the turnoff because only a very small fraction of the lost matter from the primary is accreted by the secondary. All the possible candidates contributing to BSs in M67 from FGB+MS are low-mass binaries, since the secondaries from intermediate-mass FGB+MS binaries have left the main sequence at 4 Gyr. For a $2M_\odot$ star, the minimum mass of the secondary is about $1.6M_\odot$ for $\beta = 0.0$ and $M_c = 0.25M_\odot$. The stars with this mass have left the main sequence in the old open cluster.

Different from the case of FGB+MS, the BSs resulting from EAGB+MS and TPAGB+MS have similar orbital periods for various β (see Figs. 15 and 16). Meanwhile, the mass difference of the BSs from different β is also not as obvious as that from FGB+MS binaries. **In the cases of EAGB+MS and TPAGB+MS, some BSs have masses similar to those from FGB+MS, and some have lower masses, when β is larger than 0.1. The lower mass BSs mix with those from β with lower than the given value. Stellar wind may account for this consequence. When the primary evolves from FGB to EAGB, then to TPAGB, its mass becomes less and less due to stellar wind. Correspondingly, the minimum mass of the MS companion for stable mass transfer also becomes smaller. The companions may then have lower masses after RLOF with evolution. As a result, the masses of blue stragglers in Figs. 15 and 16 extend to lower values than those in Fig. 14.**

From the **criteria** of the polytropic model and Hurley et al. (2002), only long-orbital period BSs (with orbital period greater than 1600 d) may be produced from giants transferring matter to the MS companions. Since case A and early case B (the mass donor is during Hertzsprung gap at the onset of RLOF) mass transfer are only responsible for some short- and mid-period BSs (up to 100 d, Chen & Han, 2004), there seems to be a period gap of hundreds days from the two **criteria** above. However, this period gap will not appear from the criterion of this paper. The BSs from different giant binaries cover the period range from several days to thousands of days (see Figs. 14 to 16).

As an example, we show the mass ratio versus the mass of BSs for the case of TPAGB+MS binaries at the onset and at the termination of RLOF in Fig. 17. From the figure, we see that the mass ratio at the onset of RLOF is located in a triangle region, where the upper boundary is determined by the dynamical instability and the lower boundary is determined by the mass of the accretor after the RLOF.

We have not included example 3 in section 4 in the above study. Systematic investigation for this case is difficult at present, since we have little knowledge of the condi-

tions for binaries to avoid CE during initially dynamically unstable RLOF. The conditions are possibly relevant to the parameters such as the mass (and the core mass) of the primary, the mass ratio of the components, the orbital period etc.. Furthermore, it may also be affected by the detailed process of mass transfer. The study of the conditions is beyond the scope of **this** paper. If case 3 is a real case, only a very small fraction (less than 1 per cent) from those with dynamically unstable RLOF is enough to produce BSs in M67. The products here have much longer main-sequence lives in comparison to those from dynamically stable RLOF, since the secondaries in general have much lower mass due to the initially large mass ratio (greater than q_c) and are less evolved before RLOF. From Table 5, we see that at $t = 2.47\text{Gyr}$, a star with $1.5M_\odot$ has already formed and it becomes a BS when $t > 2.5\text{Gyr}$.¹³ The material around the BSs might give us some clues on their parent stars.

5.4 Comparison to Observations

Several works focus on the BSs in M67 from observations (Milone & Latham 1992; Ahumada & Lapasset 1995; Sandquist & Shetrone 2003). In the new catalogue of BSs in open clusters (Ahumada & Lapasset 2007), there are 30 BSs in this old open cluster. Since **there is** no orbital information for these BSs in Ahumada & Lapasset (2007), the main observational data we adopted here are from some earlier studies.

Milone & Latham (1992) reported the radial velocities for 13 BSs in the open cluster M67 according to observations **over** about 9 years. Three of the 13 BSs rotate too rapidly to allow reliable velocity determinations (Latham & Milone 1996). Among the ten BSs left, only one (F190) shows a short orbital period, about 4.2 d, while five **have** long-orbital periods in the range from 800 to 5000 d. The other four BSs are considered as single stars by some studies (e.g Hurley et al., 2001). Three of the five long-orbital period BSs have obvious orbital eccentricities and the other two are in near-circular orbits. Sandquist & Shetrone (2003) presented an analysis of the time series photometry of M67 for W UMa systems, BSs and related objects. There are 24 possible BSs observed in their study and most of them show no variation in **their** light curves. Two BSs, S968 and S1263, which **were** considered as single stars before, are possible variables in the study of Sandquist & Shetrone (2003).

The BSs resulting from the criterion of Hurley et al. (2002) have orbital periods beyond 1600 d ($\log P > 3.2$ as seen in Fig. 13). However, four of the five observed long-orbital period BSs have orbital periods less than this value. The simulation from the polytropic model **gives** a similar result. The BSs from the criterion of this paper may well cover the orbital period range, but it seems that none of the five BSs is from the mass transfer between an FGB and a MS, since the smallest orbital period is 846 d ($\log P = 2.93$), which is far greater than the maximum orbital period resulting from the FGB+MS binaries, as seen in Fig. 14. The BSs with mid orbital period (i.e. from tens of days to hundreds of days) are possibly from **FGBs transferring matter to**

¹³ The age $t = 2.5\text{Gyr}$ is for a cluster with a turnoff of around $1.5M_\odot$.

their MS companions, but it needs more observational evidence to confirm the existence of these BSs.

The orbital eccentricity is a puzzle from mass transfer, since the orbit should be circularized by tidal interaction of the two components of a binary, which is just undergoing, or after, RLOF. Some studies considered that dynamical collision is necessary to explain the observed orbital eccentricities. Recently, Marinovic et al. (2007) found that, due to the enhanced mass loss of the AGB component at orbital phases closer to the periastron, the net eccentricity growth rate in one orbit is comparable to the rate of tidal circularisation in many cases. They reproduced the orbital period and eccentricity of the Sirius system with this eccentricity enhancing mechanism. Their study provides an explanation for the eccentricities of long-orbital period BSs without dynamical collision.

6 DISCUSSIONS AND CONCLUSIONS

Our study shows that the critical mass ratio, q_c , for dynamically stable mass transfer between a giant star and a MS companion depends on the stellar radius at the onset of mass transfer. For **any given** mass, a more evolved star is less stable for RLOF, since the evolutionary timescale for a more evolved star is shorter and hence the mass transfer rate is higher than that for **less-evolved ones**. The results including stellar wind (Han et al. 2002) are consistent with the tendency in this paper, except for **cases where** $M_{1i} = 0.8M_\odot$, which have a larger f_c and a larger q_c in comparison to those of $M_{1i} \geq 1.0M_\odot$. The behaviour of the cases of $M_{1i} = 0.8M_\odot$ here is similar to the consequences of a polytropic model. Meanwhile, from Table 3 in the paper of Han et al. (2002), we see that, *at a similar core mass, binaries* with a low primary mass (or a large f_c) **have larger** q_c , **also** consistent with equation(1) except for the binaries with $M_{1i} = 1.9M_\odot$. Our results for $\beta = 0$ in this paper **match those** of Han et al. (2002) (see the upper panel of Fig.9). Due to the various core masses, however, the dependence of q_c on f_c is completely scattered as shown in the upper panel of Fig.9. So, it is very likely that both M_c and f_c have influences on q_c , but the effect is different for binaries **of different** masses, i.e. M_c dominates the case **where** the primary's mass is larger than $1M_\odot$ while f_c is critical for the less **massive** ones. The thickness of the envelope might be an important cause here and the transition is possibly a gradual process. The non-monotonic behaviour of $M_{1i} = 1.9M_\odot$ results from the low degeneracy degree of the core in **primaries** with this mass.

From the criterion in this paper, we obtained some BSs with intermediate orbital period when β is less than 0.4. However, there is no one reported at present located in the orbital period range from FGB+MS binaries, as we compare our results to observations. There might be two factors for this contradiction. One is the fact that the mass of the BSs formed from such a low β is very close to the turnoff of M67, making them hard to distinguish from normal stars around the turnoff (as seen in Figure 14). The other might be that the value of β is substantially larger than 0.1 during mass transfer between FGB stars and MS companions in a real case, so few

BSs are produced in this way. Orbital determinations (in the future) might provide some constraints on the value of β . For example, since the products of FGB+MS have a wide range of orbital periods, from several days to hundreds of days, there would be some BSs with intermediate orbital periods (if β is low enough), which are possibly absent from the criterion of Hurley et al. (2002).

The possibility that a main sequence star becomes a BS via wind accretion was first suggested by Williams (1964). This idea lacked attention for a long time, since an isolated star can hardly accrete enough matter to become a BS. However it is likely different if the main sequence star is bound in a binary system where the primary is undergoing a large mass loss. In general, the mass loss rate of stellar wind is in the range of $10^{-2}M_\odot\text{yr}^{-1}$ to $10^{-6}M_\odot\text{yr}^{-1}$ as a star approaches the tip of the AGB, and some fraction of the lost material (up to 10 per cent, Tom et al. 1996) is probably accreted by its companion. This means that the secondary may significantly increase its mass when the primary undergoes a large mass loss at the tip of the AGB. Although the mass increase is likely not enough to produce a BS, the secondary still has chances to obtain matter from the primary in the following stable RLOF if it happens. So BSs with very long orbital periods (greater than 1000 days) are likely the consequences of both RLOF and wind accretion.

In this paper we present an example of a binary which avoids CE formation from initially dynamically unstable RLOF and eventually evolves to a BS with a long orbital period. We only assume that a CE has not formed in the initially dynamically unstable RLOF, but no critical conditions are shown. How to discriminate whether a CE has developed or not during this phase is unclear, as mentioned in section 5. Many parameters, such as the mass (and the core mass) of the primary, the mass ratio of the components, the orbital period etc. are relevant to this condition, which is also affected by the detailed process of mass transfer. The study of this will be **complex** and difficult, while interesting. As long as the possibility of this case exists, only a very **small fraction of systems** with dynamically unstable RLOF may provide an important contribution to BSs.

Mass transfer efficiency, β , is an important parameter. Both the criterion of dynamical instability, q_c , and the final mass of the accretor, M_a (**which are the two critical characters to determine the formation of a BS**) are relevant to this parameter. From our simulation for M67, the peak of the contribution from FGB+MS binaries is **probably** about $\beta = 0.1$, with which the BS mass is near $1.3M_\odot$. With the increase of β , the orbital period decreases and the BS mass increases, as was explained in section 5. However it is unclear **what the value of β is** in binaries. In general, β will be very small for RLOF in binaries with a giant mass donor and a compact companion (Han et al. 2002). So M_a will not be very large, **similar to the turnoff mass**.

The detailed evolution calculations in the paper show that q_c decreases with the stellar radii of the primaries at the onset of RLOF, except for cases at or near the base of the giant branch, where the core is not very degenerate and the envelope is not yet fully convective. Non-conservative assumptions will strongly affect q_c while stellar wind before mass transfer has little influence on it. To conveniently use the result we give a fit of q_c as a function of the stellar

radius of the primary at the onset of RLOF, and of the mass transfer efficiency during RLOF. Theoretically, dynamically stable mass transfer occurs once the mass ratio is less than the critical **value**. However, it is delayed in real binaries. Usually the stable mass transfer occurs after the reversion of the mass ratio.

The Monte Carlo simulations show that some binaries with the mass donor **on** the first giant branch, which have no contributions to the blue stragglers from the earlier **criteria**, will contribute to this population with the criterion obtained in this paper. Meanwhile, from our criterion, the blue stragglers resulting from the mass transfer between an AGB star and a MS companion may be more numerous and have a wider range of orbital periods than those **formed from previous criteria**. Although the result from our criterion may well cover the observed orbital period range, it seems that none of the five observed long-orbital period BSs is from the mass transfer between an FGB and a MS companion.

7 ACKNOWLEDGMENTS

The authors thank the referee for his useful suggestions on this paper and R. S. Pokorny for his improvement of the English in the manuscript. This work is supported by the Chinese National Science Foundation (Grant Nos. 10603013 and 10433030, 10521001 and 2007CB815406) and the Chinese Academy of Sciences (Grant No. O6YQ011001).

REFERENCES

- Alexander D. R., Ferguson J. W., 1994, *ApJ*, 437, 879
 Andronov N., Pinsonneault M. H., Terndrup D. M., 2006, *ApJ*, 646, 1160
 Ahumada J., Lapasset E., 1995, *A&AS*, 109, 375
 Ahumada J., Lapasset E., 2007, *A&A*, 463, 789
 Beer M. E., Dray L. M., King A. R., Wynn G. A., 2007, *MNRAS*, 375, 1000
 Bloeker T., 1995, *A&A*, 279, 727
 Bonatto Ch., Bica E., 2003, *A&A*, 405, 525
 Carraro G., Girardi L., Bressan A., Chiosi C., 1996, *A&A*, 305, 849
 Caughlan G. R., Folwer W. A., 1988, *At. Data Nucl. Data Tables*, 40, 284
 Caughlan G. R., Folwer W. A., Harris M. J., Zimmerman B. A., 1985, *At. Data Nucl. Data Tables*, 35, 198
 Chen X., Han Z., 2004, *MNRAS*, 355, 1182
 Chen X., Han Z., 2008, *MNRAS*, 384, 1263
 Chen X., Han Z., 2007, *ChJAA*, 7, 245 (No.2)
 Davies M. B., Piotto G., De Angeli F., 2004, *MNRAS*, 349, 129
 De Macro, O., Lanz, T., Ouellette, J. A., Zurek, D., Shara, M. M., 2004, *ApJ*, 606, L151
 Eggleton P.P., 1971, *MNRAS*, 151, 351
 Eggleton P.P., 1972, *MNRAS*, 156, 361
 Eggleton P.P., 1973, *MNRAS*, 163, 179
 Eggleton P.P., 1983, *ApJ*, 268, 368
 Eggleton P.P., Fitchett M. J., Tout C. A., 1989, *ApJ*, 347, 998
 Fan X. et al., 1996, *AJ*, 112, 628
 Ferraro F. R., Sills A., Rood R. T., Paltrinieri B., Buonanno R., 2003, *ApJ*, 588, 464
 Friel E. D., Janes K. A., 1993, *A&A*, 267, 75
 Han, Z.; Eggleton, P.P.; Podsiadlowski, Ph.; Tout C.A.; 1995, *MNRAS*, 277, 1443
 Han, Z.; Eggleton, P.P.; Podsiadlowski, Ph.; Tout C.A.; Webbink, R.F., 2001, *ASP Conf. Ser.*, 229, pp205-216
 Han Z., Podsiadlowski Ph., 2006, *MNRAS*, 368, 1095
 Han Z., Podsiadlowski Ph., Eggleton P.P., 1994, *MNRAS*, 270, 121
 Han Z., Podsiadlowski Ph., Maxted P. F. L., Marsh T. R., Ivanova N., 2002, *MNRAS*, 336, 449
 Hjellming M. S., Webbink R. F., 1987, *ApJ*, 318, 794
 Hobbs L. M., Thorburn J. A., 1991, *AJ*, 102, 1071
 Hurley J. R., Pols O. R., Aarseth S. J., Tout C. A., 2005, *MNRAS*, 363, 293
 Hurley J. R., Pols O. R., Tout C. A., 2000, *MNRAS*, 315, 543
 Hurley J. R., Pols O. R., Tout C. A., 2002, *MNRAS*, 329, 897
 Hurley J. R., Tout C. A., Aarseth S. J., Pols O. R., 2001, *MNRAS*, 323, 630
 Iben I. Jr., Renzini A., 1983, *ARA&A*, 21, 271
 Iglesias C. A., Rogers F. J., 1996, *ApJ*, 464, 943
 Itoh N., Adachi T., Nakagawa M., Kohyama Y., Munakata H., 1989, *ApJ*, 339, 354
 Itoh N., Mutoh H., Hikita A., Kohyama Y., 1992, *ApJ*, 395, 622
 Janes K. A., Phelps R. L., 1994, *AJ*, 108, 1773
 Kippenhahn R., Weigert A., 1967, *Z. Ap.*, 65, 251
 Latham D. W., Milone A. A. E., 1996, in Milone E. F., Mermilliod J.-C., eds, *ASP Conf. Ser. Vol.90, The Origins, Evolution, and Destinies of Binary Stars in Clusters*, Vol.7. Astron. Soc. Pac., San Francisco, p.385
 Lejeune T., Cuisinier F., Buesel R., 1997, *A&AS*, 125, 229
 Lejeune T., Cuisinier F., Buesel R., 1998, *A&AS*, 130, 65
 Leonard P. J. T., 1996, 470, 521
 Mapelli M., Sigurdsson S., Colpi M. et al. 2004, *ApJ*, 605, L29
 Marinovic A. A. B., Glebbeek E., Pols O. R., 2007, *astro-ph0710.4859*
 Mateo M., Harris H., Nemec J., Olszewski E., 1990, *AJ*, 100, 469
 Mazeh T., Goldberg D., Duquennoy A., Mayor M., 1992, *ApJ*, 401, 265
 Mc Crea W. H., 1964, *MNRAS*, 128, 147
 Meng X., Chen X., Han Z., 2007, [astro-ph]arXiv:0706.3581
 Miller G. E., Scalo J. M., 1979, *ApJS*, 41, 513
 Milone A. A. E., Latham D. W., 1992, in Kondo Y., Sistero R. F., Polidan R. S., eds, *Pro. IAU Symp. 151, Evolutionary processes in Interacting Binary Stars*, Vol. 7. Kluwer, Dordrecht, p.473
 Paczynski B., 1965, *Acta Astr.*, 15, 89
 Podsiadlowski Ph., Joss P. C., Hsu J. J. L., 1992, *MNRAS*, 391, 246
 Podsiadlowski Ph., Rappaport S., Pfahl E., 2002, *ApJ*, 565, 1107
 Pols O.R., Schröder K.-P., Hurley J.R., Tout C.A., Eggleton P.P., 1998, *MNRAS*, 298, 525
 Pols O.R., Tout C.A., Eggleton P.P., Han Z., 1995, *MNRAS*, 274, 964
 Pols O. R., Marnus M., 1994, *A&A*, 288, 475
 Reimers D., 1975, *Mem. R. Soc. Liege*, 6e, Ser., 8, 369
 Renzini A., 1981, in Chiosi C., Stalio R., eds, *Effects of Mass Loss on Stellar Evolution*. Reidel, Dordrecht, p.319
 Sandquist E. L., Shetrone M. D., 2003, *AJ*, 125, 2173
 Schröder K.-P., Pols O. R., Eggleton P. P. 1997, *MNRAS*, 285, 696
 Scott J. K., Webbink R. F., 1984, *ApJ*, 279, 252
 Soberman G. E., Phinney E. S., van den Heuvel E. P. J., 1997, *A&A*, 327, 620
 Stryker L. L., 1993, *PASP*, 105, 1081
 Tom T., Henri M. J. B., Alain J., 1996, *MNRAS*, 280, 1264
 Tout C. A., Aarseth S. J., Pols O. R., Eggleton P. P., 1997, *MNRAS*, 291, 732
 Xin Y., Deng L., 2005, *ApJ*, 619, 824
 VandenBerg D. A., Stetson P. B., 2004, *PASP*, 116, 1012
 Webbink R. F., 1988, in *The Symbiotic Phenomenon*, eds.

J. Mikolajewska, M. Friedjung, S. J. Kenyon & R. Viotti
(Kluwer: Dordrecht), p.311
Williams I. P., 1964, MNRAS, 128,389